Targeting topoisomerase II with trypthantrin derivatives: Discovery of 7-((2-(dimethylamino)ethyl)amino)indolo[2,1-b]quinazoline-6,12-dione as an antiproliferative agent and to treat cancer

Targeting Topoisomerase II with Trypthantrin Derivatives: Discovery of 7-((2-(dimethylamino)ethyl)amino)indolo[2,1-*b*]quinazoline-6,12-dione as an Antiproliferative Agent and to Treat Cancer

Elena Catanzaro,[a,l] Nibal Betari,[a,l] Jose M. Arencibia,[b] Serena Montanari,[a] Claudia Sissi,[c] Angela De Simone,[d] Ivano Vassura,[e] Alan Santini,[a] Vincenza Andrisano,[a] Vincenzo Tumiatti,[a] Marco De Vivo,[b] Dmitri V. Krysko,[f,g,h] Marco B.L. Rocchi,[i] Carmela Fimognari,[a]* Andrea Milelli [a]**

[a] Department for Life Quality Studies, Alma Mater Studiorum-Università di Bologna, Corso d'Augusto 237, 47921 Rimini, Italy.

[b] Molecular Modeling and Drug Discovery Lab, Istituto Italiano di Tecnologia, Via Morego 30, 16163 Genova, Italy.

[c] Department of Pharmaceutical and Pharmacological Sciences, University of Padova, Via Marzolo, 5, 35131, Padova, Italy.

[d] Department of Drug Science and Technology, University of Turin, Via Giuria 9, 10125 Torino.

[e] Department of Industrial Chemistry "Toso Montanari", Alma Mater Studiorum-Università di Bologna, Viale del Risorgimento, 4, 40136, Bologna, Italy.

[f] Cell Death Investigation and Therapy Laboratory, Department of Human Structure and Repair, Ghent University, 9000 Ghent, Belgium.

[g] Cancer Research Institute Ghent, 9000 Ghent, Belgium.

[h] Department of Pathophysiology, Sechenov First Moscow State Medical University, 119146 Moscow, Russia.

[i] Department of Biomolecular Sciences, Campus Scientifico "E. Mattei", University of Urbino Carlo Bo, Via Ca' Le Suore 2, Urbino, Italy.

[l] These two authors contributed equally to the work.

Corresponding Authors:

* carmela.fimognari@unibo.it

** andrea.milelli3@unibo.it

Abstract

Drugs targeting human topoisomerase II (topoII) are used in clinical practice since decades. Nevertheless, there is an urgent need for new and safer topoII inhibitors due to the emergence of secondary malignancies and the appearance of resistance mechanisms upon treatment with topoII-targeted anticancer drugs. In the present investigation, we report the discovery of a new topoII inhibitor, whose design was based on the structure of the natural product trypthantrin, a natural alkaloidal compound containing a basic indoloquinazoline moiety. This new topoII inhibitor, here numbered compound **5**, is found to inhibit topoII with an IC_{50} of 26.6 ± 4.7 µM. Notably, compound **5** is more potent than the template compound trypthantrin, and even than the widely used topoII-targeted clinical drug etoposide. In addition, compound **5** also exhibits high water solubility, a promising antiproliferative activity on different tumor cell lines such as acute leukemia, colon, and breast cancer. In light of these results, compound **5** represents a promising lead for developing new topoII inhibitors as anti-cancer therapeutic agents.

Graphical Abstract

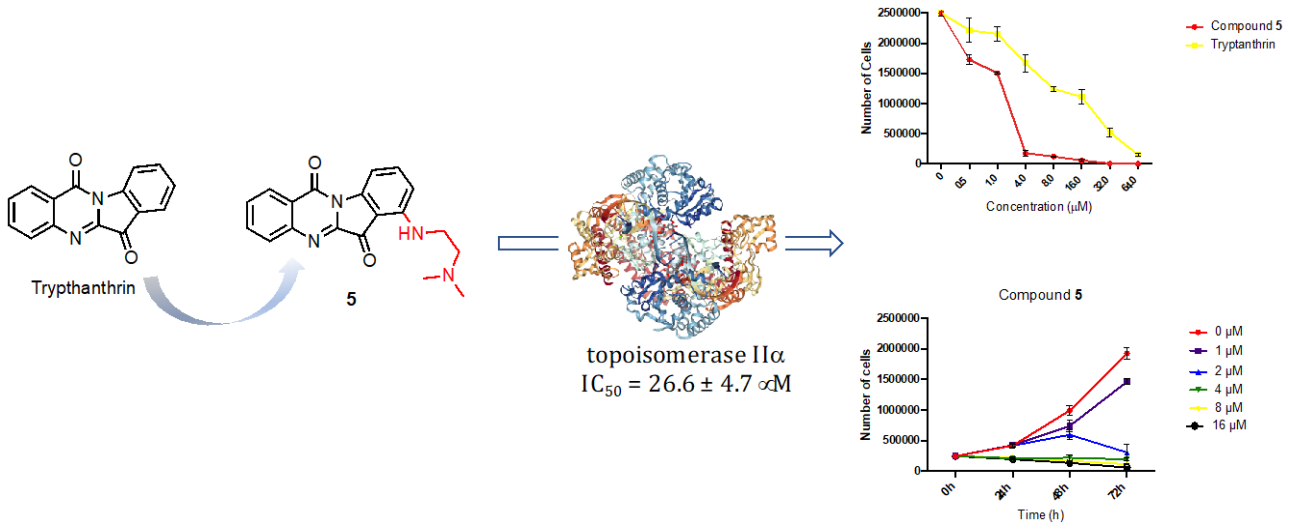

Highlights

- There is an urgent need for new and safer topoisomerase II inhibitors
- Compound **5**, a tryptanthrin derivative, is a catalytic inhibitor of topoisomerase II
- Compound **5** exhibits antiproliferative activity on different tumor cell lines
- Compound **5** blocks the cell cycle of CCRF-CEM in the G2 phase and induces DNA DSB
- Compound **5** is water soluble and shows promising in-silico ADME properties

1. Introduction

Natural products represent one of the principal sources of biologically active compounds and have been used for centuries to treat a vast range of maladies[1, 2], with prominent applications in anticancer drug discovery[3]. In this regard, important anticancer clinical drugs such as etoposide – derived from the natural product podophyllotoxin – exert their effects by blocking the activity of topoisomerase (topo) enzymes[4]. Topo, classified as type I and type II in humans, are ubiquitous enzymes that are essential in the regulation of DNA topology[5]. Type I topo performs its regulatory functions by cleaving only one strand of DNA, while Type II cleaves both DNA strands. In case of the latter, human cells encode for two isoforms, α and β, which share almost 70% sequence identity. Notably, the α isoform is predominantly expressed in highly proliferating cells, while the β isoform is mainly expressed in non-proliferating cells such as cardiac cells and neurons.

TopoII inhibitors are divided into two classes based on the mechanism of inhibition: i) "poisons", such as etoposide and doxorubicin, which trap the covalent topoII/DNA cleavage complex, leading to DNA damage and cell death; and ii) "catalytic inhibitors", such as novobiocin and merbarone, which act by preventing the enzyme from performing its functions, without generation of DNA damage[6, 7].

Recently, Kwon and coworkers reported that Benzo[*b*]tryptanthrin, a benzo annulated derivative of tryptanthrin, acts as a DNA non-intercalative catalytic topoI/II inhibitor and exerts cytotoxic effects in human cancer cell lines.[8] Tryptanthrin is an indoloquinazoline alkaloid that displays several biological actions[9]. For instance, it is a potent indoleamine 2,3-dioxygenase inhibitor with activity in Lewis lung cancer tumor-bearing mice[10] and exerts anti-angiogenic effects by reducing the VEGF-induced Tyr1175 phosphorylation of VEGFR2 to the control level[11].

Here, we report the discovery of 7-((2-(dimethylamino)ethyl)amino)indolo[2,1-*b*]quinazoline-6,12-dione (**5**) as a new catalytic topoII inhibitor endowed with promising antiproliferative activity of cancer cells. Compound **5** emerged from a small set of trypthantrin analogs (Figure 1) designed with the aim of a) fine-tuning the drug-target ionic and H-bonding interactions and b) increasing the water solubility of the derivatives, since tryptanthrin suffers of low water solubility[12]. It is worth noting that compounds **1-12** are newly designed tryptanthrin analogues and, therefore, their synthesis and topoII inhibitory activities are not previously reported. Due to its topoII inhibition profile, we further characterized compound **5** to clarify its mechanism of action.

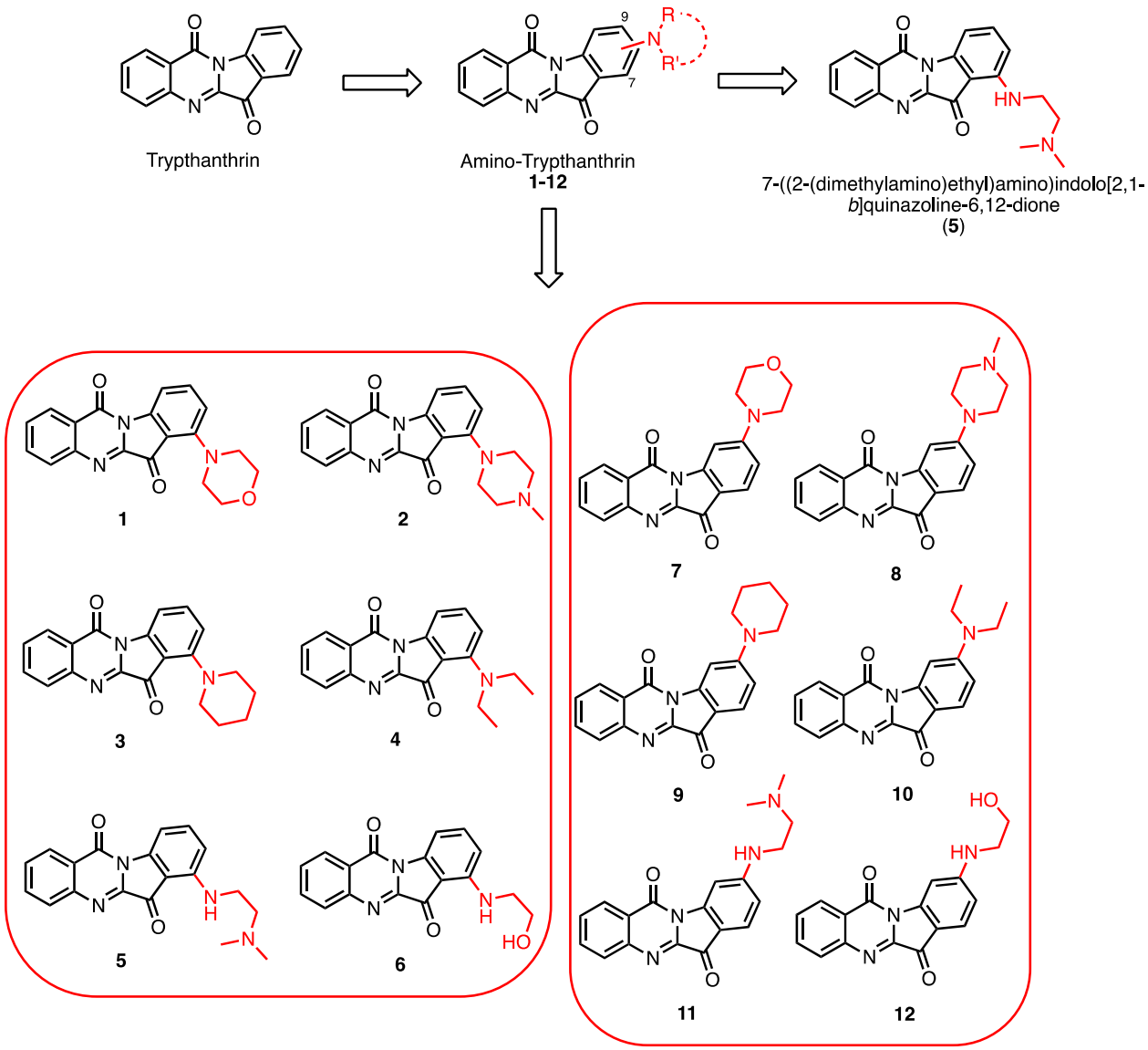

Figure 1. Design and structures of target compounds **1-12**.

2. Results and Discussions

2.1 Chemistry

Synthetic strategy leading to compounds **1-12** is reported in Scheme 1. Bromo-substituted tryptanthrin (**16**, **17**) were synthesized by reacting commercially available isatoic anhydride **13** and appropriate bromoisatin **14** or **15**[13] in the presence of triethylamine. Classic nucleophilic substitution between the bromo-substituted Trypthantrin **16**, **17** and the appropriate amine led to the target compounds **1-12**. Unfortunately, we were not able to synthesize compounds **11** and **12**.

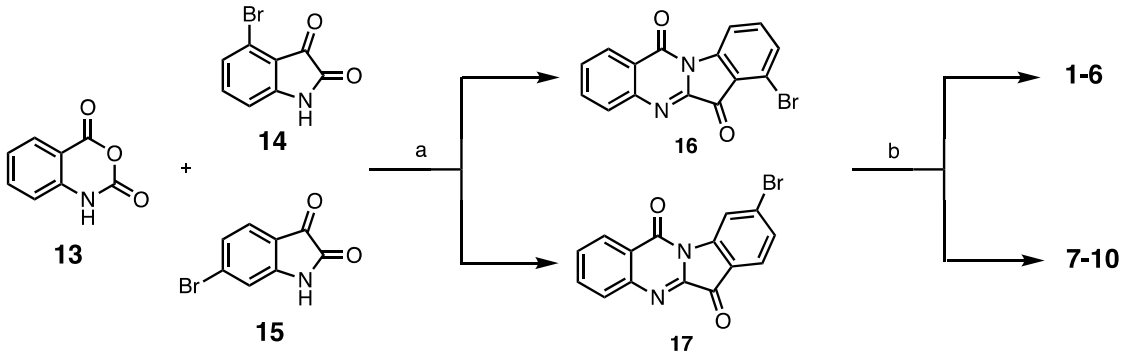

Scheme 1. a) Et_3N (1 eq.), toluene, 6h, reflux (yields: **16**: 75%, **17**: 67%): b) amine (1 eq.), DMF, 3h, 70°C (yields: 49-71%).

2.2 Topoisomerase II inhibition

Evaluation of the effects of the compounds on human topoIIα activity was measured using a decatenation assay (Table 1, Figure 2 and 1SI). Compound **5** was the most potent and inhibited topoII with an IC_{50} of 26.6 ± 4.7 µM. This activity was about 2.5 times better than that observed under the same experimental conditions for etoposide (68.3 ± 5.4 µM), which was used as positive control. Furthermore, trypthantrin turned out to be ineffective under our experimental conditions. Thus, the activity of **5** seems due to the presence of an additional N atom in the lateral chain, such as in compounds **2** and **8** (Table 1, Supplementary Figures 1 and 2). In compound **5**, the *N*,*N*-dimethyl alkylamine seems critical to form interactions with the enzyme to generate its inhibitory effect.

Then, we performed a cleavage assay of pBR 322 by topoIIα in the presence/absence of increasing concentrations of compound **5.** No stabilization of the cleavage complex was observed, indicating that compound **5** acted as a topoIIα inhibitor rather than a poison.

Table 1. IC_{50} values of etoposide, tryptanthrin and its derivatives **1-10** on the activity of human DNA topoII.

Compound	IC_{50} (µM)	Compound	IC_{50} (µM)
Etoposide	68.3 ± 5.4	**5**	26.6 ± 4.7
Tryptanthrin	n.e.	**6**	n.e.
1	n.e.	**7**	n.e.
2	114.0 ± 56.9	**8**[a]	137.5 ± 16.5
3	n.e.	**9**	n.e.
4	n.e.	**10**	n.e.

Results are the mean ± SD of two independent assays.
n.e.: no effect up to 250 µM.
[a]: 5% DMSO final concentration in the assay

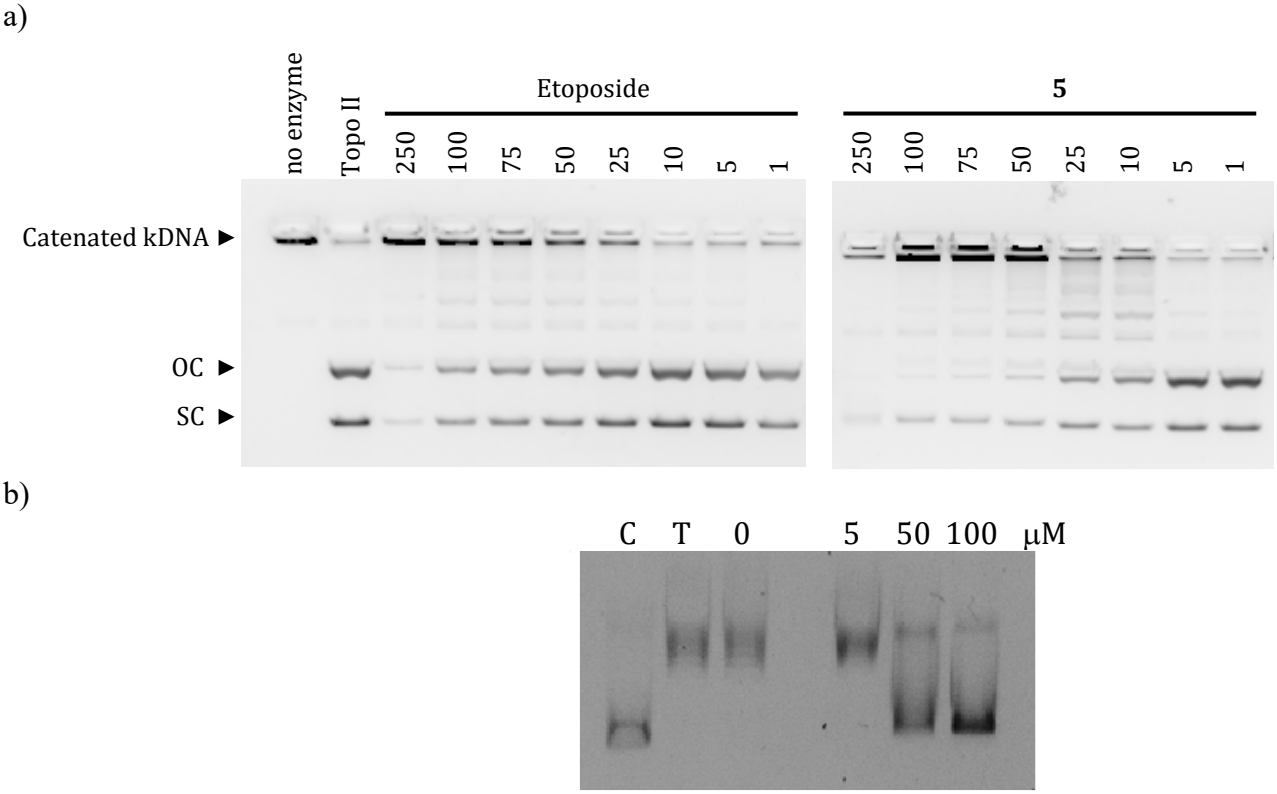

Figure 2. a) Inhibition of topoII by etoposide and compound **5**. Decatenation of kDNA by topoII (0.125 U) was performed in the presence of the indicated test compounds or 2.5% DMSO as control (Topo II lane). Products were resolved by 1 % gel electrophoresis containing SYBRsafe DNA stain. Compound concentrations (µM) are indicated above each lane. OC: Open nicked Circles; SC: Supercoiled Circles. b) Cleavage assay of pBR 322 by topoIIα in the presence/absence of increasing concentrations of compound **5**. Lane C corresponds to the plasmid in the absence of the enzyme, lanes T and 0 correspond to the plasmid treated with topoIIα and loaded before and after treatment with SDS-PK solution, respectively.

2.3 Antiproliferative activity and mechanism of action

Compound **5** was also evaluated for its ability to act as an antiproliferative agent on cancer cells. To this aim, compound **5** was assessed on seven human cancer lines from three different tumor models (leukemia, colon, and breast cancer). In all tested cell lines, it promoted a dose-dependent decrease in cell viability (Figure 3). The IC_{50} was not significantly dissimilar between cell lines except on Jurkat and MCF7, which turned out be less sensible to compound **5**. For these two compounds, the IC_{50} was up to more than a 2- and 3-fold difference in value, respectively, than the mean of all other IC_{50} recorded (around 9 µM) (Table 2). Of note, compound **5** was equally potent on a camptothecin-resistant leukemia cell line (CEM/C2), and on its non-resistant counterpart (CCRF-CEM) (Figure 3, Table 2). The occurrence of resistance is a crucial limiting factor in cancer therapy[14-16]. In this regard, this result suggests that compound **5** may indeed lead to a broad-spectrum anticancer action, which further underlines its potential for positive future developments. Also, the IC_{50} values were

comparable among cell lines and, since suspension cells represent the gold standard for flow cytometry analysis, we choose CCRF-CEM to proceed with the following studies.

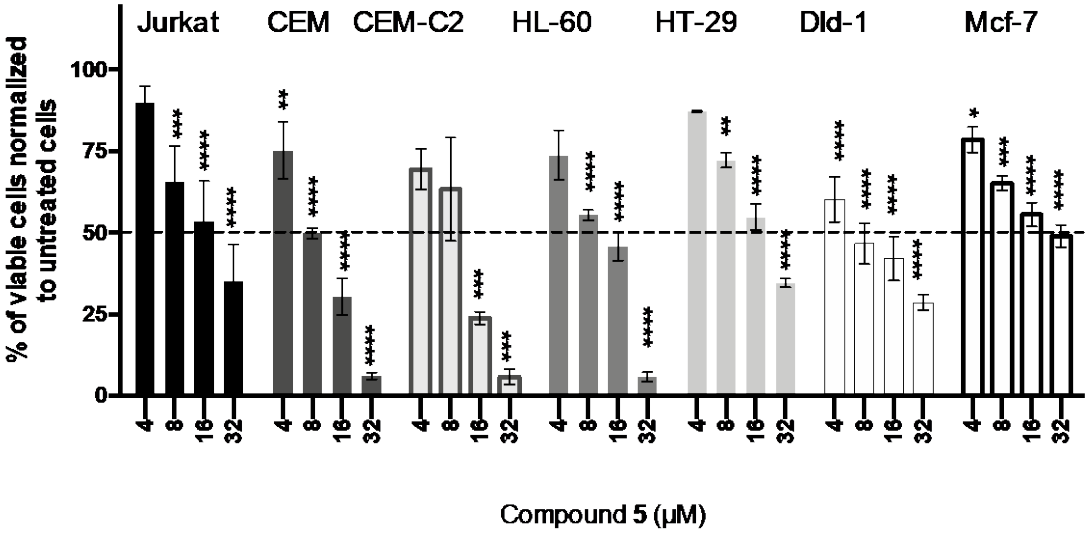

Figure 3. Percentage of viable cells normalized to untreated cells after 72h treatment with compound **5**. *P < 0.05; **P < 0.01; ***P < 0.001; ****P < 0.0001 *versus* untreated cells. Broken line indicates 50% cell viability.

Table 2. IC_{50} values obtained for the selected cell lines treated with compound **5** for 72h.

Tumor type	Cell line	IC_{50} 72h (µM)
Leukemia	Jurkat	18.20
	CCRF-CEM	8.26
	CEM/C2	9.16
	HL-60	11.46
Colon	HT-29	9.40
	Dld-1	7.13
Breast	MCF-7	30.48

We compared compound **5** cytotoxic and cytostatic potential to that of tryptanthrin. We found that compound **5** had a cytotoxic potency almost 5 times higher than that of tryptanthrin (IC_{50} 72h: 44.36 µM) (Figure 4A). To further quantify the cytostatic potential, the number of cells after 72h treatment with compound **5**, or tryptanthrin, has been counted, and we found a stronger effect of compound **5** (GI_{50} 72h: 1.36 µM) compared to that of tryptanthrin (GI_{50} 72h: 14.47 µM, Figure 4B).

It is interesting to notice that, conversely to compound **5** cytotoxicity, which prompts after 72h (Figure 4C), the cytostatic effect occurs at a concentration lower than its IC_{50} (4 µM) already after 24h treatment (Figure 4D), which corresponds to the doubling time of CCRF-CEM.

These data suggest that cells die as a consequence of the cell-cycle arrest likely induced by topoII inhibition. To test this hypothesis, we analyzed and characterized the antiproliferative properties of compound **5** and its ability to promote DNA double-strand breaks (DSB). Precisely, we assessed in which cell-cycle phase compound **5** promoted the arrest of the cell cycle; then, we investigated whether the formation of DNA DSB escorted the block and cell death was a cause or a consequence of the DNA DSB.

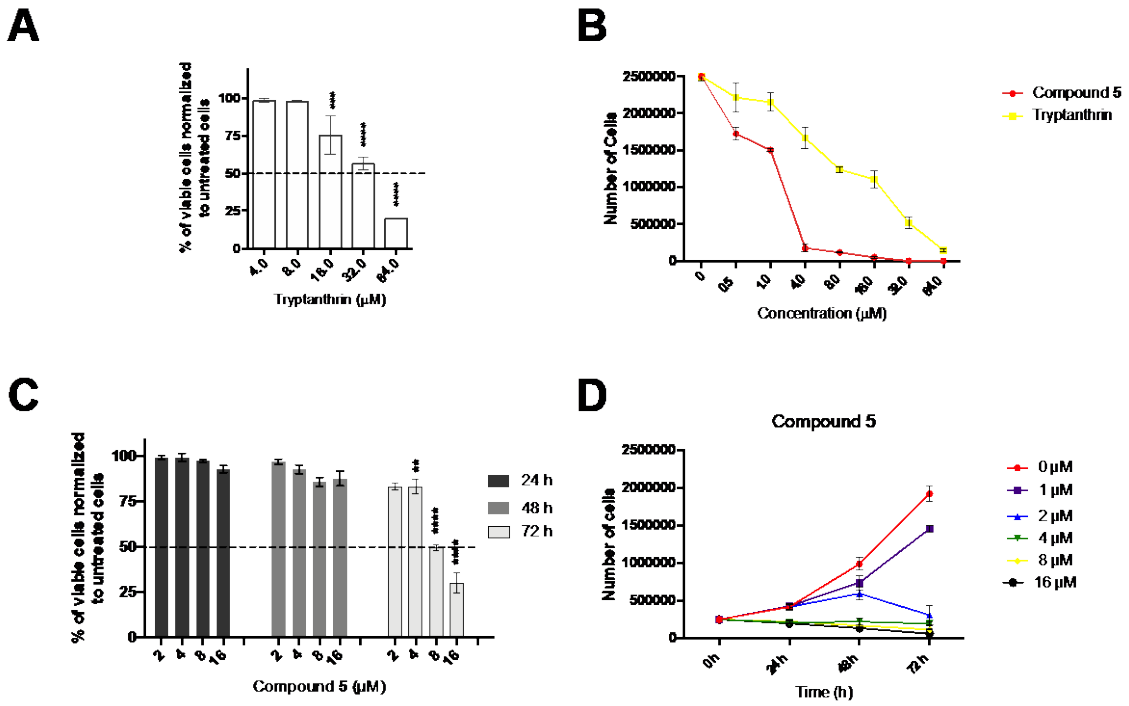

Figure 4. Percentage of viable CCRF-CEM cells normalized to untreated cells after 72h treatment with tryptanthrin (A); number of CCRF-CEM cells after 72h treatment with compound **5** or tryptanthrin (B and D); percentage of viable CCRF-CEM normalized to untreated cells after 24, 48 or 72h treatment with compound **5** (C). **P < 0.01; ***P < 0.001; ****P < 0.0001 *versus* untreated cells. Broken line indicates 50% cell viability.

One of the main functions of topoII is to decatenate sister chromatids during the G2 phase in order to allow their separation before entry into the mitotic phase (M). Thus, if the topoII activity is inhibited, a cell-cycle shutdown in phase G2 occurs, which persists until the resolution of the so-called decantation block. PI staining of permeabilized cells allows the analysis of cell distribution in the subG0, G0-G1, S, and G2-M phases of the cell cycle through the quantification of nuclear DNA[17-19]. Treatment with compound **5** produced a dose-dependent accumulation of cells in the G2/M phase, along with a related decrease in the G0-G1 population (Figure 5A and B). After 24h treatment

with **5**, 8 µM, 78% of cells were in G2/M compared to 27% of untreated cells, and no sign of cells death were recorded. When compound **5** was removed from the cell culture, and cells were cultured in complete medium for 24 additional hours (recovery condition), cells were not able to re-enter the cell cycle and consequently they died, as demonstrated by the increase in cells with fragmented DNA, *i.e.*, subG0 cells (Figure 5C and D). This evidence suggests that the damage provoked by compound **5** is not repairable.

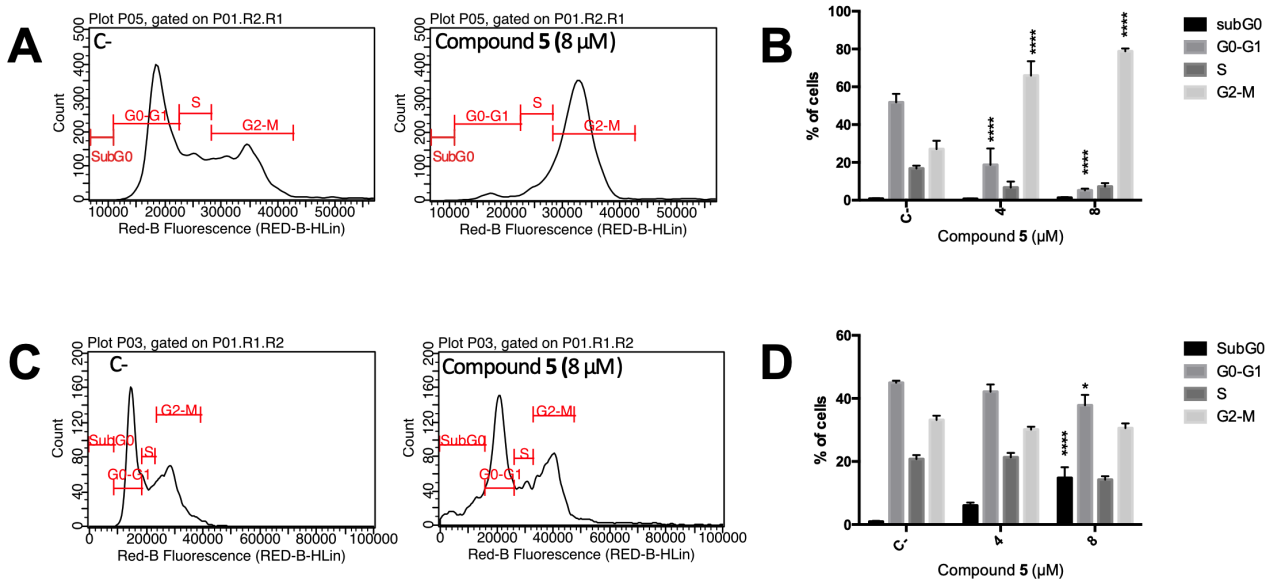

Figure 5. Cytograms (A) and histograms (B) of cell-cycle distribution after CCRF-CEM treatment with compound **5** for 24h. Cytograms (C) and histograms (D) of cell-cycle distribution after CCRF-CEM treatment with compound **5** for 24h and recovery in drug-free complete medium for additional 24h. *P < 0.05; ***P < 0.001; ****P < 0.0001 *versus* untreated cells.

To determine whether the cells treated with compound **5** accumulated in G2 or M phase, the expression of cyclins A and B was monitored. Cyclin A synthesis starts during the S-phase of the cell cycle and reaches the peak in phase G2 before being degraded during the transition from G2 to M. Cyclin B instead is expressed from phase G2, and substantially accumulates before cells enter mitosis[20, 21]. Compound **5** at the concentration of 8 µM caused a time-dependent increase in the expression of cyclin B in the G2-M phase cells, from 6h of treatment up to 24h, meaning that cells blocked in phase G2 continue to collect cyclin B1 that cannot be destroyed. Cyclin A, on the other hand, in the same step of the cell cycle (G2-M) was not modulated (Figure 6). This trend matches the effects of amsacrine, an inhibitor of topoII, on acute lymphoblastic leukemia cells, which causes a block of the cell cycle in phase G2[20] and validates the hypothesis that compound **5** acts in the same way.

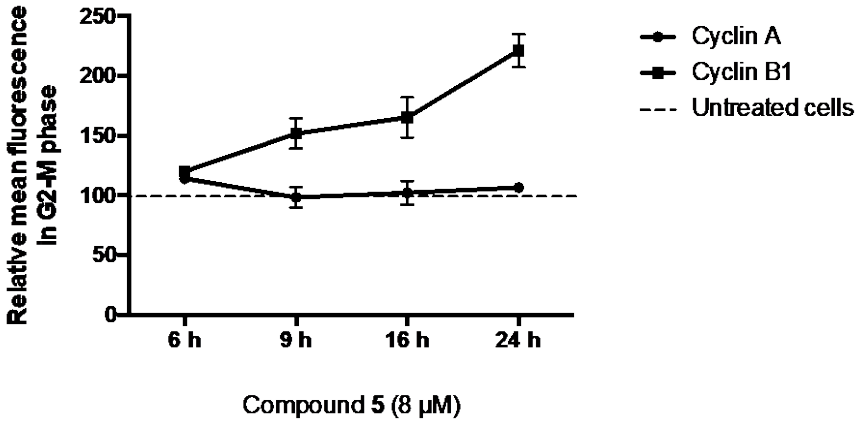

Figure 6. Relative expression of cyclin A and B1 of CCRF-CEM cells treated with 8 µM of compound **5**, as a function of time treatment. *P < 0.05; **P < 0.01; ****P < 0.0001 *versus* untreated cells

To confirm that the antiproliferative activity of compound **5** was due to the ability to block topoII, we studied its ability to induce double-strand DS DNA damage. Indeed, topo inhibitors can cause the stabilization of the topo-DNA complexes. This favors the collision between the replication fork and these stabilized complexes, leading to the stop of the replicative fork. The result is the conversion of these complexes into DS DNA lesions[22]. We linked the expression of the phosphorylated histone H2AX (γ-H2AX), the most common marker for DNA DSB, with the cell-cycle position at different time points. TopoI inhibitors produce a striking increase in the expression of γ-H2AX during the S phase, followed by G2-M and G1. TopoII inhibitors promote the DNA DSB mostly during the G1 phase, followed by S and G2-M phases[23]. Figure 7 shows that compound **5** at the concentration of 8 µM promoted an increase in γ-H2AX that perfectly fits with the latter pattern, supporting the evidence that compound **5** inhibits topoII in cells.

Moreover, this data is in agreement with the above-mentioned ability of compound **5** to kill CEM/C2 cells, which are characterized by a mutation at the catalytic site of topoI but have a functional topoII machinery[24] and turn the full circle.

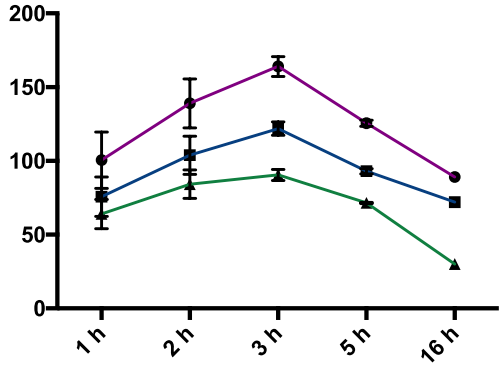

Figure 7. Changes in mean γ-H2AX immunofluorescence of CCRF-CEM cells treated with 8 μM of compound **5**, as a function of time treatment and cell-cycle phase. **P < 0.01; ***P < 0.001; ****P < 0.0001 *versus* untreated cells.

2.4 Water solubility and physicochemical properties predicted

With the aim to depict the "drug-likeness" profile of compound **5**, we first evaluated its water solubility compared to trypthantrin. In particular a value of 22.60 μg/mL (91.02 μM) was obtained for tryptanthrin while for compound **5** a solubility value of 333.04 μg/mL (996.45 μM) was detected. Thus, the results showed a ten times higher solubility for compound **5** compared to trypthantrin (Table 3). In silico prediction of some pharmacokinetic and ADME properties of compound **5** were obtained from SwissADME[25, 26], an online web tool, and displayed in Table 3. As it can be observed, compound **5** fulfills the requirements for the Lipinsky rule of Five and it is predicted to be GI absorbed and to not be a P-gp substrate. Furthermore, very importantly, compound **5** is not identified as PAINS[27].

Table 3. Water solubility and in silico pharmacokinetic data for Trypthantrin and compound **5**.

	Trypthantrin	Compound **5**		Trypthantrin	Compound **5**
Water Solubility	22.60 μg/mL	333.04 μg/mL	Log $P_{o/w}$[a]	2.22	1.81
MW[a]	248.24	334.37	GI absorption[a]	High	High
Rotable bonds[a]	0	4	BBB permeant[a]	Yes	Yes
H-bond A[a]	3	4	P-gp substrate[a]	No	No
H-bond D[a]	0	1	Lipinsky[a]	Yes	Yes
MR[a]	70.77	97.40	PAINS[a]	No	No
TPSA[a]	51.96	67.23	LeadLikeness[a]	1 violation	Yes

[a] obtained from http://www.swissadme.ch/, access date 12/04/2020.

3. Conclusions

Despite topo inhibitors are among the most popular agents used in clinical, no new inhibitors have successfully completed clinical trials in the last two decades[6]. There is an urgent need for new Topo inhibitors due to appearance of resistance and toxic effects. Indeed, most of the topo inhibitors used in therapy are poisons and long-term treatment is frequently associated with side effects, such as cardiomyopathy, development of secondary malignancies or appearance of resistance mechanisms. Indeed, ternary complex promotes the formation of DNA DSB leading to apoptosis in transformed

and normal cells. A possible strategy to overcome such drawbacks is related to the use of catalytic inhibitors that blocks the enzyme activity without the toxic effects induced by the formation of the ternary complex. Indeed, catalytic topoII inhibitors kill cancer cells and exhibit lower toxicity on normal cells and lower risk of secondary malignancies. In the present investigation, we reported about the discovery of catalytic topoII inhibitor based on the structure of natural product trypthantrin. Compound **5** inhibited topoIIα with an IC_{50} of 26.6 ± 4.7 μM, higher than that of etoposide and trypthantrin, and exhibited a promising antitumor potential on different cancer models such as acute leukemia, colon, and breast cancer cell lines. We determined that its antiproliferative mechanism of action relies on the same ability to inhibit the topoII enzyme demonstrated in the *in vitro* experiments. Indeed, our findings showed that compound **5** blocked the cell cycle of CCRF-CEM in the G2 phase and induced DNA DSB before cells underwent cell death in the characteristic way of topoII inhibitors[28-30]. Moreover, our data showed that the cytotoxic and the pronounced cytostatic effects of compound **5** were much stronger than those of tryptanthrin and pave the way to further studies to deepen its molecular mechanism of action. Since tryptanthrin has a safe profile[31] and compound **5** interacts with the α isoform of topoII enzyme, it will also be interesting to assess the actual toxicological profile of compound **5**. Because topoIIα is overexpressed in cancer cells, it represents an optimal target for antiblastic drugs[32]. Thus, if compound **5** would prove to be topoIIα–selective, it could represent an alternative to the current topo inhibitors used in the clinics, which adverse effects often hamper their therapeutic potential. However, it is not yet defined whether topoIIα and topoIIβ play dissimilar roles in the cytotoxic response to etoposide or other topoII inhibitor drugs[32]. Moreover, for most of the pre-clinical topoII inhibitors under investigation, activity testing against topoIIβ was not reported[33].

Importantly, compound **5** shows high water solubility and favorable calculated pharmacokinetic and ADME properties.

Based on these findings, compound **5** might be considered a promising hit compound to develop new catalytic topoII inhibitors. Specific experiments to analyze its toxic potential and hit-to-lead optimization studies are currently ongoing and will be reported in due course.

4. Experimental Section

4.1 Chemistry.

All the commercially available reagents and solvents were purchased from Sigma-Aldrich (St. Louis, MO, USA), Alpha Aesar (Haverhill, MA, USA), VWR (Radnor, PA, USA), and TCI , which were used without further purification. Reactions were followed by analytical thin layer chromatography

(TLC) on precoated TLC plates (layer 0.20 mm silica gel 60 with a fluorescent indicator UV254, from Sigma-Aldrich). Developed plates were air-dried and analyzed under a UV lamp (UV 254/365 nm), $KMnO_4$ stain. Nuclear magnetic resonance (NMR) experiments were run on Varian VXR 400 (400 MHz for ^1H, 100 MHz for ^{13}C). Chemical shifts (δ) are reported in parts per million (ppm) relative to tetramethylsilane (TMS) as internal reference and coupling constants (J) are reported in hertz (Hz). The spin multiplicities are reported as s (singlet), br s (broad singlet), d (doublet), t (triplet), q (quartet), and m (multiplet). Mass spectra were recorded on a VG707EH-F apparatus, and electrospray ionization (ESI) both in positive and negative mode was applied. Compounds were named following IUPAC rules as applied by ChemBioDraw Ultra (version 17.0). All of the final compounds showed ≥95% purity by elemental analysis.

4.1.1 General Procedure for the synthesis of 1-10: to a solution of the appropriate bromotryptanthrin **16** or **17** (1 eq.) in DMF, potassium carbonate (1 eq.) and the corresponding amines (1.2 eq.) were added and the resulting mixture was refluxed for 3h. The solvent was removed in vacuo and the obtained residue was purified through flash chromatography.

4.1.1.1 7-morpholinoindolo[2,1-b]quinazoline-6,12-dione **(1).** Compound **1** was obtained from compound **16** (0.1 g, 0.30 mmol), potassium carbonate (0.041 g, 0.30 mmol), morpholine (0.03 mL, 0.37 mmol). Yield: 52%. ^1H NMR (400 MHz, $CDCl_3$): δ 3.41 (t, 4H, *J* = 4.8 Hz), 3.96-3.94 (t, 4H, *J* = 4.6 Hz), 6.66 (d, 1H, *J* = 8.4), 7.52 (t, 1H, *J* = 8.0 Hz), 7.59 (td, 1H, *J* = 10.8, 1.2 Hz), 7.79 (td, 1H, *J* = 7.2, 1.6 Hz), 7.96 (d, 1H, *J* = 8.0 Hz), 8.05 (d, 1H, *J* = 7.6 Hz), 8.37 (dd, 1H, *J* = 8.0, 1.2 Hz); ^{13}C NMR (100 MHz, $CDCl_3$): δ 51.0, 66.7, 108.5, 110.4, 115.1, 123.3, 127.3, 129.4, 130.1, 134.8, 139.9, 144.2, 146.8, 147.1, 151.6, 158.0, 178.2; HRMS (ESI): $C_{19}H_{16}N_3O_3$ $[M + H]^+$: calcd 334.1192, found 334.1208.

4.1.1.2 7-(4-methylpiperazin-1-yl)indolo[2,1-b]quinazoline-6,12-dione **(2).** Compound **2** was obtained from compound **16** (0.1 g, 0.30 mmol), potassium carbonate (0.041 g, 0.30 mmol), morpholine (0.04 mL, 0.37 mmol). Yield: 61%. ^1H NMR (400 MHz, $CDCl_3$): δ 2.12 (s, 3H), 2.47 (t, 4H, *J* = 7.2 Hz), 3.55 (t, 4H, *J* = 7.4 Hz), 6.62 (d, 1H, *J* = 8.2), 7.59 (t, 1H, *J* = 8.0 Hz), 7.64 (td, 1H, *J* = 10.8, 1.0 Hz), 7.82 (td, 1H, *J* = 7.4, 1.4 Hz), 7.95 (d, 1H, *J* = 8.0 Hz), 8.07 (d, 1H, *J* = 7.4 Hz), 8.34 (dd, 1H, *J* = 8.2, 1.2 Hz); ^{13}C NMR (100 MHz, $CDCl_3$): δ 55.5, 51.7, 57.7, 108.1, 110.9, 115.0, 123.1, 128.0, 129.5, 131.0, 135.2, 140.6, 143.8, 146.0, 147.7, 152.2, 158.6, 178.0; HRMS (ESI): $C_{20}H_{19}N_4O_2$ $[M + H]^+$: calcd 347.1508, found 347.1532.

4.1.1.3 7-(piperidin-1-yl)indolo[2,1-b]quinazoline-6,12-dione **(3).** compound **3** was obtained from compound **16** (0.15 g, 0.46 mmol), potassium carbonate (0.063 g, 0.46 mmol), piperidine (0.04 mL, 0.55 mmol). Yield: 66%. ^{1}H NMR (400 MHz, $CDCl_3$): δ 1.71-1.76 (m, 6H), 3.86 (t, 4H, *J* = 7.2 Hz), 6.67 (d, 1H, *J* = 8.4), 7.45 (t, 1H, *J* = 8.0 Hz), 7.60 (td, 1H, *J* = 10.8, 1.2 Hz), 7.85 (td, 1H, *J* = 7.7, 1.2 Hz), 7.92 (d, 1H, *J* = 8.0 Hz), 8.01 (d, 1H, *J* = 7.2 Hz), 8.34 (dd, 1H, *J* = 8.2, 1.2 Hz); ^{13}C NMR (100 MHz, $CDCl_3$): δ 23.5, 24.1, 56.9, 107.9, 111.1, 115.6, 123.5, 127.9, 129.0, 131.4, 134.8, 140.9, 143.5, 146.6, 148.0, 152.5, 159.0, 178.9; HRMS (ESI): $C_{20}H_{18}N_3O_2$ $[M + H]^+$: calcd 332.1399, found 332.1381.

4.1.1.4 7-(diethylamino)indolo[2,1-b]quinazoline-6,12-dione **(4).** Compound **4** was obtained from compound **16** (0.10 g, 0.31 mmol), potassium carbonate (0.042 g, 0.31 mmol), diethylamine (0.04 mL, 0.37 mmol). Yield: 71%. ^{1}H NMR (400 MHz, $CDCl_3$): δ 1.20 (t, 6H, *J* = 7.0 Hz), 3.46 (q, 4H, *J* = 7.2, 6.8 Hz), 6.61 (d, 1H, *J* = 8.4), 7.41 (t, 1H, *J* = 8.2 Hz), 7.61 (td, 1H, *J* = 10.8, 1.4 Hz), 7.79 (td, 1H, *J* = 7.6, 1.0 Hz), 7.89 (d, 1H, *J* = 8.0 Hz), 8.11 (d, 1H, *J* = 7.0 Hz), 8.30 (dd, 1H, *J* = 8.2, 1.2 Hz); ^{13}C NMR (100 MHz, $CDCl_3$): δ 17.1, 46.5, 108.1, 111.8, 114.9, 123.9, 128.3, 129.5, 131.1, 134.1, 141.5, 143.6, 147.7, 149.4, 153.4, 159.7, 179.5; HRMS (ESI): $C_{19}H_{18}N_3O_2$ $[M + H]^+$: calcd 320.1399, found 321.1416.

4.1.1.5 7-((2-(dimethylamino)ethyl)amino)indolo[2,1-b]quinazoline-6,12-dione **(5).** Compound **5** was obtained from compound **16** (0.10 g, 0.31 mmol), potassium carbonate (0.042 g, 0.31 mmol), *N*,*N*-dimethylethylenediamine (0.04 mL, 0.37 mmol). Yield: 56%. ^{1}H NMR (400 MHz, $CDCl_3$): δ 2.35 (s, 6H), 2.65 (t, 2H, J = 6.8 Hz), 3.45 (t, 2H, J = 6.0 Hz), 6.60 (d, 1H, *J* = 8.8 Hz), 7.48 (t, 1H, *J* = 8.0 Hz), 7.62 (td, 1H, *J* = 8.0, 1.2 Hz), 7.67 (brs, 1H exch with D_2O), 7.69 (d, 1H, 7.2 Hz), 7.81 (td, 1H, *J* = 7.2, 1.6 Hz), 8.00 (d, 1H, *J* = 7.6 Hz), 8.27 (dd, 1H, *J* = 8.2, 1.2 Hz); ^{13}C NMR (100 MHz, $CDCl_3$): δ 40.4, 45.4, 57.6, 104.5, 105.7, 109.9, 123.2, 127.3, 129.2, 130.1, 134.6, 139.8, 144.7, 145.4, 146.8, 149.2, 158.2, 180.6; HRMS (ESI): $C_{19}H_{19}N_4O_2$ $[M + H]^+$: calcd 335.1508, found 335.1533.

4.1.1.6 7-((2-hydroxyethyl)amino)indolo[2,1-b]quinazoline-6,12-dione **(6).** Compound **6** was obtained from compound **16** (0.10 g, 0.30 mmol), potassium carbonate (0.042 g, 0.31 mmol), ethanolamine (0.03 mL, 0.37 mmol). Yield: 49%. ^{1}H NMR (400 MHz, DMSO-*d*): δ 3.43 (t, 2H, *J* = 6.0 Hz), 3.61-3.65 (m, 2H), 4.97 (t, 1H), 6.77 (d, 1H, *J* = 9.2 Hz), 7.51 (t, 1H, *J* = 8.2 Hz), 7.60 (td, 1H, *J* = 8.0, 1.2 Hz), 7.67 (d, 1H, 7.5 Hz), 7.80 (td, 1H, *J* = 7.2, 1.2 Hz), 7.91 (d, 1H, *J* = 7.6 Hz), 8.42 (dd, 1H, *J* = 8.0, 1.2 Hz); ^{13}C NMR (100 MHz, DMSO-d_6): δ 47.1, 62.0, 103.7, 107.9, 112.3, 122.3, 128.5, 129.2, 130.0, 131.4, 135.1, 138.9, 144.1, 147.3, 150.1, 158.5, 179.8; HRMS (ESI): $C_{17}H_{14}N_3O_3$ $[M + H]^+$: calcd 308.1035, found 308.1027.

4.1.1.7 9-morpholinoindolo[2,1-b]quinazoline-6,12-dione **(7).** Compound **7** was obtained from compound **17** (0.15 g, 0.46 mmol), potassium carbonate (0.063 g, 0.46 mmol), morpholine (0.05 mL, 0.55 mmol). Yield: 55%. ^{1}H NMR (400 MHz, $CDCl_3$): δ 3.31 (t, 2H, *J* = 4.4 Hz), 3.58 (t, 2H, 4.4 Hz), 3.90 (t, 2H, *J* = 5.0 Hz), 3.93 (t, 2H, *J* = 4.6 Hz), 6.73 (dd, 1H, *J* = 8.8, 2.4 Hz), 7.65-7.70 (m, 1H), 7.79 (d, 1H, *J* = 8.8 Hz), 7.85-7.88 (m, 1H), 8.03 (d, 1H, *J* = 8.4 Hz), 8.10 (d, 1H, *J* = 2.4 Hz), 8.39-8.43 (m, 1H); ^{13}C NMR (100 MHz, $CDCl_3$): δ 51.3, 64.0, 106.5, 107.9, 108.4, 121.1, 127.4, 128.1, 129.5, 130.5, 131.7, 133.6, 148.5, 152.4, 155.6, 161.1, 182.1; HRMS (ESI): $C_{19}H_{16}N_3O_3$ [M + H]$^+$: calcd 334.1192, found 334.1209.

4.1.1.8 9-(4-methylpiperazin-1-yl)indolo[2,1-b]quinazoline-6,12-dione **(8).** Compound **8** was obtained from compound **17** (0.10 g, 0.46 mmol), potassium carbonate (0.042 g, 0.30 mmol), *N*-methylpiperazine (0.03 mL, 0.37 mmol). Yield: 60%. ^{1}H NMR (400 MHz, $CDCl_3$): δ 2.36 (s, 3H), 2.45 (t, 4H, *J* = 7.0 Hz), 3.57 (t, 4H, *J* = 7.2Hz) 6.77 (dd, 1H, *J* = 8.6, 2.2 Hz), 7.59-7.67 (m, 1H), 7.84 (d, 1H, *J* = 8.4 Hz), 7.95-7.99 (m, 1H), 8.07 (d, 1H, *J* = 8.4 Hz), 8.12 (d, 1H, *J* = 2.6 Hz), 8.45-8.48 (m, 1H); ^{13}C NMR (100 MHz, $CDCl_3$): δ 46.6, 53.4, 58.7, 106.0, 107.5, 108.1, 121.8, 127.0, 127.9, 129.7, 130.7, 132.0, 133.9, 149.8, 153.1, 156.2, 161.7, 183.5; HRMS (ESI): $C_{20}H_{19}N_4O_2$ [M + H]$^+$: calcd 347.1508, found 347.1495.

4.1.1.9 9-(piperidin-1-yl)indolo[2,1-b]quinazoline-6,12-dione **(9).** Compound **9** was obtained from compound **17** (0.15 g, 0.30 mmol), potassium carbonate (0.063 g, 0.46 mmol), *N*-methylpiperazine (0.05 mL, 0.55 mmol). Yield: 67%. ^{1}H NMR (400 MHz, $CDCl_3$): δ 1.70-1.77 (m, 6H), 3.56-3.60 (m, 4H), 6.81 (dd, 1H, *J* = 7.8, 2.4 Hz), 7.26-7.62 (m, 1H), 7.70 (d, 1H, *J* = 8.8 Hz), 7.78-7.82 (m, 1H), 7.98 (d, 1H, *J* = 8.0 Hz), 8.18 (d, 1H, *J* = 2.4 Hz), 8.33-8.35 (m, 1H); ^{13}C NMR (100 MHz, $CDCl_3$): δ 23.1, 26.6, 56.9, 104.2, 108.6, 108.9, 118.9, 126.2, 128.9, 129.6, 130.3, 131.3, 137.0, 150.5, 154.2, 157.1, 163.5, 182.0; HRMS (ESI): $C_{20}H_{18}N_3O_2$ [M + H]$^+$: calcd 332.1399, found 332.1424.

4.1.1.10 9-(diethylamino)indolo[2,1-b]quinazoline-6,12-dione **(10).** Compound **10** was obtained from compound **17** (0.10 g, 0.30 mmol), potassium carbonate (0.042 g, 0.30 mmol), *N*-methylpiperazine (0.03 mL, 0.37 mmol). Yield: 65%. ^{1}H NMR (400 MHz, $CDCl_3$): δ 0.99 (t, 6H, *J* = 7.2 Hz), 3.67 (q, 4H, *J* = 7.4, 7.0 Hz), 6.72 (dd, 1H, *J* = 7.6, 2.4 Hz), 7.219-7.51 (m, 1H), 7.63 (d, 1H, *J* = 8.4 Hz), 7.73-7.80 (m, 1H), 7.95 (d, 1H, *J* = 7.8 Hz), 8.09 (d, 1H, *J* = 2.2 Hz), 8.37-8.43 (m, 1H); ^{13}C NMR (100 MHz, $CDCl_3$): δ 11.7, 41.5, 101.7, 107.9, 110.1, 117.0, 124.4, 127.6, 128.5, 130.6, 132.6, 138.3, 150.4, 152.3, 158.6, 162.4, 181.5; HRMS (ESI): $C_{19}H_{18}N_3O_2$ [M + H]$^+$: calcd 320.1399, found 320.1387.

4.1.2 7-bromoindolo[2,1-b]quinazoline-6,12-dione **(16)**. A mixture of 4-bromoindoline-2,3-dione **14** (0.30 g, 1.3 mmol), isatoic anhydride **13** (0.22 g, 1.3 mmol) and triethylamine (0.92 mL, 6.6 mmol) in toluene was stirred at reflux for 6 h. The solvent was removed in vacuo and the obtained residue was purified through flash chromatography using as eluent a mixture of dichloromethane / methanol (9.9:0.1) to give **16** as a yellow solid (yield: 75%). mp. 264–267 °C; ^{1}H NMR (400 MHz, $CDCl_3$): δ 7.35 (d, 1H, *J* = 6.6 Hz), 7.51-7.64 (m, 2H), 7.77-7.83 (m, 1H), 7.95 (d, 1H, *J* = 6.0 Hz), 8.21 (dd, 1H, *J* = 6.4, 3.0 Hz), 8.45 (d, 1H, *J* = 4.4 Hz).

4.1.3 9-bromoindolo[2,1-b]quinazoline-6,12-dione **(17)**. A mixture of 4-bromoindoline-2,3-dione **14** (0.35 g, 1.5 mmol), isatoic anhydride **13** (0.25 g, 1.5 mmol) and triethylamine (1.04 mL, 7.5 mmol) in toluene was stirred at reflux for 6 h. The solvent was removed in vacuo and the obtained residue was purified through flash chromatography using as eluent a mixture of dichloromethane / methanol (9.9:0.1) to give **16** as a yellow oil (yield: 67%). ^{1}H NMR (400 MHz, $CDCl_3$) δ 7.41 (dd, 1H, *J* = 6.8, 4.2 Hz), 7.69-7.71 (m, 1H), 7.81-7.92 (m, 2H), 8.11 (d, 1H, *J* = 4.2 Hz), 8.32 (d, 1H, *J* = 7.0 Hz), 8.65 (d, 1H, J = 6.0 Hz).

4.2 Aqueous solubility

In order to determine the aqueous solubility of both tryptanthrin and compound **5**, 400 µL of PBS solution containing 2% DMSO, were added to an excess of powder of each compound. The samples were left under continuous stirring at 25°C for 24 h. The quantification of dissolved compounds was carried out by measuring the UV spectrum of supernatant solutions obtained after centrifugation and proper dilutions. The supernatants from each sample were filtered through a 0.45 µm PTFE membrane filter. A calibration graph (Absorbance [Abs] versus concentration [µM]) was established by measuring the UV absorption of four solutions. The concentration range for solutions containing tryptanthrin was from 3 µM to 9 µM. On the other hand, the linearity for compound **5** was established in the concentration range from 2.5 µM to 20 µM. All the solutions were prepared in PBS containing 2% DMSO. The concentration of the saturated solutions was determined by the straight-line equation obtained from the calibration graphs. A solubility value expressed as µg/mL was then obtained for both the compounds.

4.3 Biology

4.3.1 Topoisomerase II assay

Evaluation of the effect of the compounds on human topoisomerase II alpha activity was measured using a decatenation assay (Inspiralis). The assay was performed following the manufacturer's instructions. Briefly, the reaction mixture containing the compound or DMSO (vehicle) was incubated for 30 min at 37°C and then resolved by electrophoresis in 1% agarose gels containing SYBR safe DNA stain (Invitrogen). Final DMSO concentration in the assay was 2.5%, except in the case of compound **8** where it was 5% due to lower solubility of the compound. After electrophoresis, the gels were scanned and the intensity of the decatenated products (Supercoiled Circles; SC) from topoisomerase activity was obtained using ImageJ software. IC_{50} values were calculated by fitting a four-parameter nonlinear regression model using GraphPad Prism software V5.03 (GraphPad Software, Inc., USA). Results are reported as the mean ± SD of two independent assays.

4.3.2 Topoisomerase IIα cleavage assay

Supercoiled pBR322 (150 ng) in the presence/absence of increasing concentration of tested compound was incubated with 5 U of Topoisomerase IIα (Inspiralis) in the provided buffer at 37 °C. After 15 min, the reaction was stopped with 0.1% SDS and 1.6 µg of proteinase K in 10mM Na-EDTA. Mixtures were kept for 30 min at 45 °C. Reaction products were resolved by 1% agarose gel in 1X TAE (10mM Tris 1mM EDTA, 0.1% acetic acid pH 8.0) buffer. At the end of the run gels were stained with ethidium bromide and were visualized on a Geliance apparatus.

4.3.3 Cell lines and treatment

Acute leukemia cells (Jurkat, HL-60, CCRF-CEM, camptothecin-resistant acute lymphoblastic leukemia CEM/C2) and DLD-1 were cultured in RPMI containing 4.5 g/L glucose and supplemented with 2 mM glutamine, 100 U/mL penicillin, 100 µg/L streptomycin and 10% heat-inactivated fetal bovine serum (FBS), except for HL-60 which needed 20% of FBS. Colorectal adenocarcinoma cells (HT-29) were cultured in McCoy's 5a with the same supplements used for the above-mentioned cell lines. Breast carcinoma cells (MCF-7) were cultured in Eagle's Minimum Essential Medium added with 0.01 mg/mL human recombinant insulin, 100 U/mL penicillin, 100 µg/L streptomycin and 10% FBS. All leukemia cell lines grow in suspension, while colon and breast cancer are adherent cells. All cell lines were cultured at 37°C under 5% CO_2.

To perform all the experiments with Jurkat, CCRF-CEM, and CEM/C2, $0.25x10^6$ cells/mL were seeded to not exceed, after 72h, the maximal cell density that guarantees an exponential growth of cells. For the same reason, $0.125\ x10^6$ cells/mL seed density has been chosen for HL-60 cells. For all adherent cell lines, $0.01x10^6$ cells were seeded per well in a 96 wells plate.

4.3.4 Viability assay

Cells were cultured for 24, 48, or 72h with increasing concentrations of compound **5** or tryptanthrin (0-64 µM). Then, for the leukemia cell lines, viability was determined by the eosin exclusion dye. Viable cells were counted using a Bürker chamber and light microscopy (Nikon Eclipse TS2, Amsterdam, Netherlands). The 4-methylumbelliferyl heptanoate (MUH; Sigma Aldrich St. Louis, MO, USA) assay was used to measure adherent cell viability. MUH becomes highly fluorescent after hydrolysis of the ester linkage and, thus, measures cellular lipase and esterase activity[34]. After cell treatment with the compounds, cells were washed with PBS and incubated with MUH 0,01 mg/mL. After 30 min of incubation at 37°C and 5% CO_2, fluorescence was measured (330 nm excitation; 450 nm emission) using the microplate reader Victor X3 (Perkin Elmer, Walthman, MA, USA). Three technical replicates for each condition were analyzed in each biological replicate. Before analyzing data, the mean of the blank was subtracted on the mean of all conditions. Then, the percentage of viable cells was calculated normalizing the fluorescence for each treatment condition on the untreated cells (negative control) using the following calculation:

$$\% \text{ of viable cells} = \frac{\text{fluorescence of treated sample}}{\text{fluorescence of negative control}} \times 100$$

To efficiently compare these results to the one obtained with the exclusion dye assay, we also normalized the % of viable leukemia cells of treated cells on the negative control.

4.3.5 Proliferation assay

CCRF-CEM were treated for 24, 48, and 72h with compound **5** or tryptanthrin. Cells were stained with eosin, and the number was determined using a Bürker chamber and light microscopy.

Cell-cycle analysis was performed on CCRF-CEM after 24h treatment with compound **5** or in the so-called "recovery condition". In the latter design, CCRF-CEM were treated for 24h with compound **5**; then the conditioned medium was removed after centrifugation, cells were washed with PBS and cultured for other 24h in complete medium.

After one or the other treatment, cells were permeabilised for at least 1h with ethanol 70% and then stained with the DNA intercalating dye propidium iodide (PI, 10 µg/mL; Thermo Fisher Scientific, Carlsbad, CA, USA) and RNAse A (100 µg/mL; Roche, Sigma Aldrich). At the end of incubation at room temperature for 20 min in the dark, samples were analyzed *via* flow cytometry.

4.3.6. Antibody staining

Cyclin A, B1, and γ-H2Ax expression was analyzed *via* flow cytometry. CCRF-CEM were treated with compound **5** 8 μM for 6, 9, 16, and 24 h or for 1, 2, 3, 5, and 16h, respectively, to measure cyclin A and B1 and γ-H2AX levels. For each condition, 1×10^6 cells were collected, fixed in 2% of paraformaldehyde (10 min), and permeabilized in 90% methanol (at least 30 min). Cells were then washed and incubated for 30 min with the corresponding primary antibody (anti-cyclin A 1:50; anti-cyclinB1 1:50 or anti-γ-H2Ax 1:40; Invitrogen, Thermo Fisher Scientific), washed in PBS and stained with the respective secondary antibody (anti-mouse 1:200; anti-rabbit 1:200; Invitrogen) for other 30 min. Cells were washed, stained with PI (10 μg/mL) and RNAse A (100 μg/mL), and after 20 min incubation analyzed *via* flow cytometry.

The relative expression of cyclin A and B1 was calculated normalizing the mean fluorescence intensity (MFI) to that of untreated cells in the G2-M phase cell, identified thanks to the PI staining. Delta γ-H2AX was calculated as previously described by Huang et al[23].

4.3.7. Flow cytometry

All flow cytometric analyses were performed using Guava EasyCyte 6 2L cytometer (Guava Technologies, Merck Millipore, Darmstadt, Germany). At least 10000 events were recorded for each sample.

4.3.8 Statistical analysis

All biological experiments were performed at least in triplicates. Results were expressed as the mean ± SEM and were analyzed by Student's *t*-test or two-way ANOVA with 0.05 significance threshold. IC_{50} (the concentration that causes 50% of cell death) and GI_{50} (the concentration that causes 50% of growth inhibition) were calculated using the non-linear regression. GraphPad Instat 6.0 statistical software (GraphPad Prism, San Diego, CA, USA) was used to perform all the analyses.

Declaration of competing interest

The authors declare that they have no known competing financial interests.

Acknowledgments

This research was supported by University of Bologna (RFO).

References

[1] D.J. Newman, G.M. Cragg, Natural Products as Sources of New Drugs from 1981 to 2014, J Nat Prod, 79 (2016) 629-661.
[2] F. Li, Y. Wang, D. Li, Y. Chen, Q.P. Dou, Are we seeing a resurgence in the use of natural products for new drug discovery?, Expert Opin Drug Discov, 14 (2019) 417-420.
[3] A. Lichota, K. Gwozdzinski, Anticancer Activity of Natural Compounds from Plant and Marine Environment, Int J Mol Sci, 19 (2018).
[4] X. Liang, Q. Wu, S. Luan, Z. Yin, C. He, L. Yin, Y. Zou, Z. Yuan, L. Li, X. Song, M. He, C. Lv, W. Zhang, A comprehensive review of topoisomerase inhibitors as anticancer agents in the past decade, Eur J Med Chem, 171 (2019) 129-168.
[5] J.C. Wang, Cellular roles of DNA topoisomerases: a molecular perspective, Nat Rev Mol Cell Biol, 3 (2002) 430-440.
[6] C. Bailly, Contemporary challenges in the design of topoisomerase II inhibitors for cancer chemotherapy, Chem Rev, 112 (2012) 3611-3640.
[7] W. Hu, X.S. Huang, J.F. Wu, L. Yang, Y.T. Zheng, Y.M. Shen, Z.Y. Li, X. Li, Discovery of Novel Topoisomerase II Inhibitors by Medicinal Chemistry Approaches, J Med Chem, 61 (2018) 8947-8980.
[8] K.Y. Jun, S.E. Park, J.L. Liang, Y. Jahng, Y. Kwon, Benzo[b]tryptanthrin inhibits MDR1, topoisomerase activity, and reverses adriamycin resistance in breast cancer cells, ChemMedChem, 10 (2015) 827-835.
[9] R. Kaur, S.K. Manjal, R.K. Rawal, K. Kumar, Recent synthetic and medicinal perspectives of tryptanthrin, Bioorg Med Chem, 25 (2017) 4533-4552.
[10] S. Yang, X. Li, F. Hu, Y. Li, Y. Yang, J. Yan, C. Kuang, Q. Yang, Discovery of tryptanthrin derivatives as potent inhibitors of indoleamine 2,3-dioxygenase with therapeutic activity in Lewis lung cancer (LLC) tumor-bearing mice, J Med Chem, 56 (2013) 8321-8331.
[11] T. Motoki, Y. Takami, Y. Yagi, A. Tai, I. Yamamoto, E. Gohda, Inhibition of hepatocyte growth factor induction in human dermal fibroblasts by tryptanthrin, Biol Pharm Bull, 28 (2005) 260-266.
[12] Y.P. Fang, Y.K. Lin, Y.H. Su, J.Y. Fang, Tryptanthrin-loaded nanoparticles for delivery into cultured human breast cancer cells, MCF7: the effects of solid lipid/liquid lipid ratios in the inner core, Chem Pharm Bull (Tokyo), 59 (2011) 266-271.
[13] P. Polychronopoulos, P. Magiatis, A.L. Skaltsounis, V. Myrianthopoulos, E. Mikros, A. Tarricone, A. Musacchio, S.M. Roe, L. Pearl, M. Leost, P. Greengard, L. Meijer, Structural basis for the synthesis of indirubins as potent and selective inhibitors of glycogen synthase kinase-3 and cyclin-dependent kinases, J Med Chem, 47 (2004) 935-946.
[14] N. Vasan, J. Baselga, D.M. Hyman, A view on drug resistance in cancer, Nature, 575 (2019) 299-309.
[15] O. Krysko, T.L. Aaes, V.E. Kagan, K. D'Herde, C. Bachert, L. Leybaert, P. Vandenabeele, D.V. Krysko, Necroptotic cell death in anti-cancer therapy, Immunol Rev, 280 (2017) 207-219.
[16] E. Catanzaro, G. Greco, L. Potenza, C. Calcabrini, C. Fimognari, Natural Products to Fight Cancer: A Focus on, Toxins (Basel), 10 (2018).
[17] P. Pozarowski, Z. Darzynkiewicz, Analysis of cell cycle by flow cytometry, Methods Mol Biol, 281 (2004) 301-311.
[18] D.V. Krysko, T. Vanden Berghe, K. D'Herde, P. Vandenabeele, Apoptosis and necrosis: detection, discrimination and phagocytosis, Methods, 44 (2008) 205-221.
[19] G. Matteo, T. Eleonora, L. Romolo, D.G. Elena, F. Lorenzo, L. Anna, S. Augusto, C. Vittorio, F. Carmela, Atmospheric Non-Equilibrium Plasma Promotes Cell Death and Cell-Cycle Arrest in a Lymphoma Cell Line, Plasma Processes and Polymers, 2015, 1354-1363.
[20] J. Gong, F. Traganos, Z. Darzynkiewicz, Discrimination of G2 and mitotic cells by flow cytometry based on different expression of cyclins A and B1, Exp Cell Res, 220 (1995) 226-231.

[21] R.J. Widrow, P.S. Rabinovitch, K. Cho, C.D. Laird, Separation of cells at different times within G2 and mitosis by cyclin B1 flow cytometry, Cytometry, 27 (1997) 250-254.
[22] H. Zhao, F. Traganos, Z. Darzynkiewicz, Kinetics of histone H2AX phosphorylation and Chk2 activation in A549 cells treated with topotecan and mitoxantrone in relation to the cell cycle phase, Cytometry A, 73 (2008) 480-489.
[23] X. Huang, F. Traganos, Z. Darzynkiewicz, DNA damage induced by DNA topoisomerase I- and topoisomerase II-inhibitors detected by histone H2AX phosphorylation in relation to the cell cycle phase and apoptosis, Cell Cycle, 2 (2003) 614-619.
[24] A. Fujimori, W.G. Harker, G. Kohlhagen, Y. Hoki, Y. Pommier, Mutation at the catalytic site of topoisomerase I in CEM/C2, a human leukemia cell line resistant to camptothecin, Cancer Res, 55 (1995) 1339-1346.
[25] A. Daina, O. Michielin, V. Zoete, SwissADME: a free web tool to evaluate pharmacokinetics, drug-likeness and medicinal chemistry friendliness of small molecules, Sci Rep, 7 (2017) 42717.
[26] http://www.swissadme.ch/.
[27] C. Aldrich, C. Bertozzi, G.I. Georg, L. Kiessling, C. Lindsley, D. Liotta, K.M. Merz, A. Schepartz, S. Wang, The Ecstasy and Agony of Assay Interference Compounds, ACS Med Chem Lett, 8 (2017) 379-382.
[28] N.A. Smith, J.A. Byl, S.L. Mercer, J.E. Deweese, N. Osheroff, Etoposide quinone is a covalent poison of human topoisomerase IIβ, Biochemistry, 53 (2014) 3229-3236.
[29] W. Manami, K. Khosuke, M. Shoko, M. Keiichi, K. Susumu, M. Shohei, 20-O-IngenolE*Z,* a catalytic topoisomerase II inhibitor, specifically inhibits cell proliferation and induces double-strand DNA breaks in B*LM* -/- cells, MedChemComm, 2011, 824-827.
[30] P. Chène, J. Rudloff, J. Schoepfer, P. Furet, P. Meier, Z. Qian, J.M. Schlaeppi, R. Schmitz, T. Radimerski, Catalytic inhibition of topoisomerase II by a novel rationally designed ATP-competitive purine analogue, BMC Chem Biol, 9 (2009) 1.
[31] H.L. Chan, H.Y. Yip, N.K. Mak, K.N. Leung, Modulatory effects and action mechanisms of tryptanthrin on murine myeloid leukemia cells, Cell Mol Immunol, 6 (2009) 335-342.
[32] A. Montecucco, F. Zanetta, G. Biamonti, Molecular mechanisms of etoposide, EXCLI J, 14 (2015) 95-108.
[33] K. Hevener, T.A. Verstak, K.E. Lutat, D.L. Riggsbee, J.W. Mooney, Recent developments in topoisomerase-targeted cancer chemotherapy, Acta Pharm Sin B, 8 (2018) 844-861.
[34] V.W. Dolinsky, D.N. Douglas, R. Lehner, D.E. Vance, Regulation of the enzymes of hepatic microsomal triacylglycerol lipolysis and re-esterification by the glucocorticoid dexamethasone, Biochem J, 378 (2004) 967-974.